Acceptor-bound phonons in cubic semiconductors

M. A. Kanehisa, D. Petritis,* and M. Balkanski
Laboratoire de Physique des Solides,† Université Pierre et Marie Curie, 4 place Jussieu, F-75230 Paris, France
(Received 9 October 1984)

The theory of impurity-electron—LO-phonon binding considered by Dean, Manchon, and Hopfield, among others, is reformulated and generalized. When there are several impurity electronic states having excitation energies comparable with the LO-phonon energy, the impurity-phonon binding energies can essentially be obtained by diagonalizing the exchange integrals among electronic ground and relevant excited states. The theory is then applied to the LO phonons bound to acceptors in cubic semiconductors, whereby the effect of valence-band degeneracy is taken into account in the spherical approximation of Baldereschi and Lipari. Compared with the coupling to the hydrogenlike impurity, binding becomes deeper because of the shrinkage of acceptor wave functions and the bound phonon states acquire fine structures which are classified according to the total momentum change in excitation. Detailed numerical calculations are carried out for ZnS, ZnSe, ZnTe, and CdTe, and compared with available experimental data on ZnTe.

I. INTRODUCTION

In intrinsic semiconductors, usually electronic excitation energies are much larger than the phonon energy and these two types of polarizations can be considered independent in the zeroth approximation. However, when, by introduction of impurities or application of a magnetic field, the electronic excitation energy is made close to the phonon energy, there appears a resonant coupling between the two systems. This coupling may give rise to a bound state due to the repetition of the energy-exchange process,

lattice polarization $\rightarrow$ electronic polarization $\rightarrow$ lattice polarization $\rightarrow \cdots$.

The simplest example of the phenomena might be the plasmon—LO-phonon coupling observed in heavily doped semiconductors.[1] The free-carrier plasmon energy can be matched resonant with the LO-phonon energy by changing the impurity concentration. In this case, the electronic excitation (plasmon) has only one degree of freedom corresponding to its translational motion (like the LO phonon) and hence, for each momentum $\mathbf{K}$, one can diagonalize the plasmon-phonon Hamiltonian. When the electronic excitation has an internal structure, the phenomenon becomes much more complicated. The exciton-phonon complex[2] of Toyozawa and Hermanson would be an example. The exciton has an internal degree of freedom (relative motion of the electron and the hole) and another class of motion (total motion), and the electron-phonon interaction mixes all these motions, making it impossible to solve analytically the integral equation describing the dynamics of the coupled system. The coupling of an impurity electron to a phonon constitutes an interesting intermediate case: The electron system has several types of excitation ($1S \rightarrow 2S$, $1S \rightarrow 2P$, etc.), but has no translational motion making the integral equation simple enough to permit an analytic solution.

The presence of impurities in the crystal often leads to the appearance of localized lattice vibrations due to the change in mass between the impurity and the host material, and also due to the change in force constant linking the impurity to the neighboring host atoms. This type of localized mode has been extensively studied for a long time,[3] and will not concern us here. Another class of local lattice oscillations in which we shall be interested seems to have been first pointed out by Kogan and Suris,[4] who showed that, when the impurity excitation energy is close to the energy of optical phonons, the interaction between them becoming appreciable, bound states may occur. In 1970, Dean, Manchon, and Hopfield[5] found a peak in Raman scattering between the TO and LO phonons in n-type GaP, and attributed it to the LO phonon bound to donors due to its dielectric effect. They also calculated the binding energies explicitly using the Fröhlich coupling, and the result, involving no adjustable parameters, could be quantitatively compared with experiments. The mechanism of impurity-phonon binding is that the change in polarizability due to the presence of an impurity electron perturbs the dielectric function locally and shifts the LO-phonon frequency. Barker[6] has proposed a macroscopic model for this mechanism, where the impurity atoms are replaced by dielectric spheres embedded in a host dielectric medium. Impurity-bound phonons have also been observed in p-type materials.[7–9] Experimental methods of observation include Raman scattering,[5,9] luminescence (as accompanying phonons),[5,7] luminescence excitation spectra,[8] and infrared measurements.[6] The microscopic theory[4,5] for impurity-bound phonons has been generalized by Rashba[10] for more than two electronic levels, but he has obtained no explicit solution. Mahanty and Paranjape[11] have considered the case of discrete lattice, which, in the continuum limit, reduces to the result of Dean *et al.*, who used the Fröhlich model. Finally, some review papers also treat the subject.[12,13]

The hydrogen model for the impurity electron does not give a satisfactory agreement when applied to acceptor-bound phonons.[8,9] This is because the degeneracy in the

 ©1985 The American Physical Society

valence band makes acceptor spectra much more complicated than donor spectra.[14] The simple hydrogenic levels split into sublevels, and the acceptor electrons are more localized and more deeply bound than the corresponding donor electrons (i.e., of the same mass parameter).[15] It is then to be expected that the phonon bound to the acceptor should also reveal this band-structure effect: fine structure and stronger binding; strong localization of electrons results in strong electron-phonon interactions.[16] It is the purpose of the present paper to analyze quantitatively the acceptor-bound phonons in cubic semiconductors. In Sec. II we shall first generalize the theory of Dean *et al.* to the case of (almost) degenerate impurity states having nearly the same energy as the LO phonon. In Sec. III the theory of acceptor states due to Baldereschi and Lipari[15] is resumed. Their theory exploits the approximate spherical symmetry satisfied by most diamond- and zinc-blende-type semiconductors, and enables one to classify acceptor spectra in a way similar to the atomic spectra, and also to calculate systematically the acceptor states as functions of the valence-band parameters. Our variational wave functions are much simpler than those used by Baldereschi and Lipari, but give energies as accurate as theirs. In Sec. IV we combine the results of the two preceding sections: our theory is applied to acceptor-bound phonons using the spherical model. We show bound phonons are classified according to the total change of momentum in excitation, K, which includes the change of the orbital angular momentum of the envelope function as well as of the "spin" of the valence band forming the acceptor states. In Sec. V we carry out numerical calculations for bound phonons in ZnS, ZnSe, ZnTe, and CdTe, and compare them with available experimental data on ZnTe. In Sec. VI we summarize our main results.

II. THEORY OF IMPURITY-PHONON BINDING

In this section we derive an integral equation for the impurity-bound phonon state and convert it into an algebraic eigenvalue problem. Let the Hamiltonian for the LO phonon interacting with an impurity (donor or acceptor) electron be

$$H=H_L+H_e+H' , \tag{2.1}$$

where H_L, H_e, and H' are the LO phonon, the impurity electron, and the interaction Hamiltonians, respectively, given by

$$H_L=\sum_{\mathbf{k}}\hbar\omega_{\mathbf{k}}a_{\mathbf{k}}^{\dagger}a_{\mathbf{k}} , \tag{2.2}$$

$$H_e=\sum_{j}|j)\varepsilon_j(j| , \tag{2.3}$$

$$H'=\sum_{\mathbf{k}}v_{\mathbf{k}}(a_{\mathbf{k}}+a_{-\mathbf{k}}^{\dagger}) . \tag{2.4}$$

Here, $|j)$ is the one-electron state with energy ε_j, and, especially, $j=0$ is the ground impurity state. The electron-phonon coupling (2.4) is of the Fröhlich type,[17] and

$$v_{\mathbf{k}}(\mathbf{r})=\left[\frac{2\pi e^2}{\bar{\epsilon}}\frac{\hbar\omega_{\mathbf{k}}}{V}\right]^{1/2}\frac{e^{i\mathbf{k}\cdot\mathbf{r}}}{k}\left[\frac{1}{\bar{\epsilon}}=\frac{1}{\epsilon_\infty}-\frac{1}{\epsilon_0}\right] , \tag{2.5}$$

where ϵ_0 and ϵ_∞ are static and optical dielectric constants, and V is the total volume of the crystal.

We designate the uncoupled phonon-electron states as $a_{\mathbf{k}}^{\dagger}|0)$ for a state with one phonon $\mathbf{k}$ and the electron in the ground state, or $a_{\mathbf{k}}^{\dagger}a_{\mathbf{k}'}^{\dagger}|j)$ for a state with two phonons $\mathbf{k}$ and $\mathbf{k}'$, and the electron in the state j. The bound-phonon state φ can be obtained by expanding it in terms of all these uncoupled states, and then by requiring it to be the eigenstate of the total Hamiltonian (2.1). Let us take the linear combination

$$\varphi=\sum_{\mathbf{k}}a_{\mathbf{k}}^{\dagger}|0)c_{\mathbf{k}}+\sum_{j>0}|j)d_j+\tfrac{1}{2}\sum_{\substack{\mathbf{k},\mathbf{k}',\\ j(>0)}}a_{\mathbf{k}}^{\dagger}a_{\mathbf{k}'}^{\dagger}|j)f_{\mathbf{k}\mathbf{k}'j}+\cdots , \tag{2.6}$$

where the first term is the free one-phonon state with the electron in the ground state, the second term is the electronic excited state without phonon, and the third term is the state with two phonons in the electronic excited state. In principle, there are higher phonon states contributing to φ, but they are ignored here since we will be mainly interested in polar semiconductors whose Fröhlich coupling constant is relatively weak. The expansion coefficients $c_{\mathbf{k}}$, d_j, and $f_{\mathbf{k}\mathbf{k}'j}$ ($=f_{\mathbf{k}'\mathbf{k}j}$, without loss of generality), are to be determined by the condition

$$H\varphi=E\varphi , \tag{2.7}$$

with the total Hamiltonian (2.1). Inserting (2.6) into (2.7) and making inner products with $(0|a_{\mathbf{k}}$, $(j|$, and $(j|a_{\mathbf{k}'}a_{\mathbf{k}}$, one obtains three equations to be solved simultaneously for $c_{\mathbf{k}}$, d_j and $f_{\mathbf{k}\mathbf{k}'j}$:

$$(E-\hbar\omega_{\mathbf{k}}-\varepsilon_0)c_{\mathbf{k}}=\sum_{j(>0)}(0|v_{-\mathbf{k}}|j)d_j+\sum_{\substack{\mathbf{k}',\\ j(>0)}}(0|v_{\mathbf{k}'}|j)f_{\mathbf{k}\mathbf{k}'j} , \tag{2.8a}$$

$$(E-\varepsilon_j)d_j=\sum_{\mathbf{k}}(j|v_{\mathbf{k}}|0)c_{\mathbf{k}} , \tag{2.8b}$$

$$(E-\hbar\omega_{\mathbf{k}}-\hbar\omega_{\mathbf{k}'}-\varepsilon_j)f_{\mathbf{k}\mathbf{k}'j}=(j|v_{-\mathbf{k}}|0)c_{\mathbf{k}'}+(j|v_{-\mathbf{k}'}|0)c_{\mathbf{k}} . \tag{2.8c}$$

Then, eliminating d_j and $f_{\mathbf{k}\mathbf{k}'j}$, one obtains, finally, an equation involving solely $c_{\mathbf{k}}$:

$$(E-\hbar\omega_{\mathbf{k}}-\tilde{\varepsilon}_0)c_{\mathbf{k}}=\sum_{\mathbf{k}'}T_{\mathbf{k}\mathbf{k}'}(E)c_{\mathbf{k}'} , \tag{2.9}$$

with

$$T_{\mathbf{k}\mathbf{k}'}(E)=\sum_{j(>0)}\left[\frac{(0|v_{-\mathbf{k}}|j)(j|v_{\mathbf{k}'}|0)}{E-\varepsilon_j}+\frac{(0|v_{\mathbf{k}'}|j)(j|v_{-\mathbf{k}}|0)}{E-\hbar\omega_{\mathbf{k}}-\hbar\omega_{\mathbf{k}'}-\varepsilon_j}\right] \tag{2.10}$$

and

$$\tilde{\varepsilon}_0=\varepsilon_0-\sum_{\mathbf{k}'j(>0)}\frac{(0|v_{\mathbf{k}'}|j)(j|v_{-\mathbf{k}'}|0)}{E-\hbar\omega_{\mathbf{k}}-\hbar\omega_{\mathbf{k}'}-\varepsilon_j} .$$

Clearly, Eq. (2.9) is an integral equation for $c_{\mathbf{k}'}$ and its

kernel (2.10) is the scattering matrix corresponding to the two processes depicted in Fig. 1. $\tilde{\varepsilon}_0$ is the renormalized electronic ground-state energy, and will be written simply ε_0 henceforth. The assumption in (2.6) of taking up to two-phonon states corresponds to taking these lowest-order diagrams. It is to be remarked, however, that we are not limited to the second-order processes when we *solve* (2.9), but that instead we taken into account infinite repetition of the elementary process (2.10); otherwise, no bound state would appear at all.

In general, Eq. (2.9) cannot be solved analytically. However, with several reasonable assumptions we can reduce it to a mathematically tractable form. First, we assume that the binding is not very strong and, hence, replace the energy E in the denominator of (2.10) by its noninteracting value $E \approx \hbar\omega_{\mathbf{k}'} + \varepsilon_0$. Second, we ignore the LO-phonon dispersion and set $\omega_{\mathbf{k}} \approx \omega_0$. Furthermore, we take real electronic wave functions, so that

$$(j \mid v_{\mathbf{k}} \mid 0) = (0 \mid v_{\mathbf{k}} \mid j) \ .$$

With these assumptions (of which, the third is not essential), (2.10) becomes

$$T_{\mathbf{k}\mathbf{k}'} = \sum_{j\,(>0)} \frac{2(\varepsilon_j - \varepsilon_0) v_{-\mathbf{k},0j} v_{\mathbf{k}',j0}}{(\hbar\omega_0)^2 - (\varepsilon_j - \varepsilon_0)^2} \ .$$

We use (2.5) to rewrite it slightly as

$$T_{\mathbf{k}\mathbf{k}'} = -\frac{4\pi e^2}{\bar{\epsilon} V} \sum_{j\,(>0)} D_j^2 \frac{(0 \mid e^{-i\mathbf{k}\cdot\mathbf{r}} \mid j)(j \mid e^{i\mathbf{k}'\cdot\mathbf{r}} \mid 0)}{kk'} \ , \tag{2.11}$$

where

$$D_j = \left[\frac{(\varepsilon_j - \varepsilon_0)\hbar\omega_0}{(\varepsilon_j - \varepsilon_0)^2 - (\hbar\omega_0)^2} \right]^{1/2} \tag{2.12}$$

is the (dimensionless) resonance denominator, and when all electronic excitation energies are larger than the LO-phonon energy (i.e., when $\varepsilon_j - \varepsilon_0 > \hbar\omega_0$), D_j is real.

In Eq. (2.11), if one can take only one state in the sum over intermediate states j, the kernel $T_{\mathbf{k}\mathbf{k}'}$ of the integral equation (2.9) becomes separable and it can be solved trivially.[5] When we are interested in the effect of excited states higher than that considered, or when there are several almost degenerate states having energies comparable with the phonon energy, one must retain the sum j in (2.11). In this case, the kernel is a sum of separable

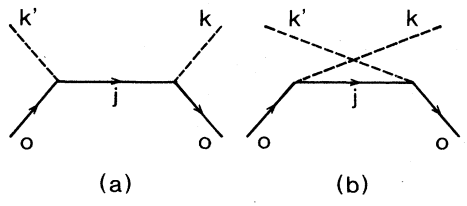

FIG. 1. Lowest-order impurity-phonon scattering processes. A phonon $\mathbf{k}'$ is scattered by an electron into a phonon $\mathbf{k}$ by virtually exciting it into j. Absorption and reemission of the phonon can be in (a) one or the (b) other order. Infinite repetition of these processes may generate bound states of the impurity and phonon.

terms and one can still solve (2.9) as follows. One multiplies (2.9) by $D_i(i \mid e^{i\mathbf{k}\cdot\mathbf{r}} \mid 0)/k$ and sums over $\mathbf{k}$ to obtain an equation for

$$\chi_i = D_i \sum_{\mathbf{k}} \frac{(i \mid e^{i\mathbf{k}\cdot\mathbf{r}} \mid 0)}{k} c_{\mathbf{k}} \ , \tag{2.13}$$

which reads

$$(E - \hbar\omega_0 - \varepsilon_0)\chi_i = -\sum_j S_{ij}\chi_j \ , \tag{2.14}$$

with

$$S_{ij} = \frac{4\pi e^2}{\bar{\epsilon} V} D_i D_j \sum_{\mathbf{k}} \frac{(i \mid e^{i\mathbf{k}\cdot\mathbf{r}} \mid 0)(0 \mid e^{-i\mathbf{k}\cdot\mathbf{r}} \mid j)}{k^2} \ . \tag{2.15}$$

Now, Eq. (2.14) is an eigenvalue equation, in which, we remember, that i and j are impurity electronic states. The matrix S_{ij} of this eigenvalue problem can be further rewritten as

$$S_{ij} = \frac{\epsilon_0}{\bar{\epsilon}} D_i D_j X_{ij} \ , \tag{2.16}$$

and

$$\begin{aligned} X_{ij} &= \int d^3r_1 \int d^3r_2 \, \psi_i^*(\mathbf{r}_1)\psi_0^*(\mathbf{r}_2) \frac{e^2}{\epsilon_0 \mid \mathbf{r}_1 - \mathbf{r}_2 \mid} \\ &\quad \times \psi_0(\mathbf{r}_1)\psi_j(\mathbf{r}_2) \\ &= (i,0 \mid [e^2/\epsilon_0 r_{12}] \mid 0,j) \end{aligned} \tag{2.17}$$

is nothing but an exchange integral among impurity states $\psi_i(\mathbf{r}) \equiv (\mathbf{r} \mid i)$, etc. Here we have used the relation

$$\frac{4\pi}{V} \sum_{\mathbf{k}} \frac{e^{i\mathbf{k}\cdot(\mathbf{r}_1 - \mathbf{r}_2)}}{k^2} = \frac{1}{\mid \mathbf{r}_1 - \mathbf{r}_2 \mid} \ .$$

Let the eigenvalue of S_{ij} be E_λ with eigenvector $\chi_{i\lambda}$:

$$\sum_j S_{ij}\chi_{j\lambda} = E_\lambda \chi_{i\lambda} \ . \tag{2.18}$$

Then, from (2.14), one has

$$E = \hbar\omega_0 + \varepsilon_0 - E_\lambda \ , \tag{2.19}$$

i.e., E_λ is the binding energy of the λth bound phonon. In this way our integral equation for the bound-phonon problem (2.9) is reduced to solving an algebraic eigenvalue equation (2.18), whose kernel (2.16) is essentially the exchange integral (2.17). The number of bound-phonon states is just the dimension of the matrix S_{ij}, which, in turn, is the number of impurity excited states considered. Equation (2.16) indicates that there are two conditions necessary for deep binding: the large resonance denominator (2.12) and large exchange integral (2.17). We shall see in subsequent sections that it is this second condition that makes phonons more deeply bound to acceptors than to donors.

Finally, let us consider the wave function of the bound-phonon state (2.6). This is determined once we know $c_{\mathbf{k}}$, since d_j and $f_{\mathbf{k}\mathbf{k}'j}$ can be expressed in terms of $c_{\mathbf{k}}$ [see Eqs. (2.8b) and (2.8c)]. By using (2.11) and (2.13),

one rewrites (2.9) as

$$(E-\hbar\omega_0-\varepsilon_0)c_{\mathbf{k}}=-\sum_{j>0}\frac{(0\,|\,e^{-i\mathbf{k}\cdot\mathbf{r}}\,|\,j)}{k}D_j\chi_j\ .$$

One then has, for the λth bound phonon,

$$c_{\mathbf{k}\lambda}=\frac{1}{E_\lambda}\sum_{j\,(>0)}\frac{(0\,|\,e^{-i\mathbf{k}\cdot\mathbf{r}}\,|\,j)}{k}D_j\chi_{j\lambda}\ , \tag{2.20}$$

where $\chi_{j\lambda}$ is the eigenvector in (2.18) and use is made of (2.19). Equation (2.20) is the probability amplitude for a crystal phonon $\mathbf{k}$ to be contained in the bound phonon λ. From Eq. (2.8b) one then obtains the "electronlike" amplitude of the bound phonon λ,

$$d_{j\lambda}=\left[\frac{\bar{\epsilon}\hbar\omega_0 V}{8\pi e^2}\right]^{1/2}\frac{1}{E-\varepsilon_j}\frac{\chi_{j\lambda}}{D_j}\ , \tag{2.21}$$

and a similar expression for $f_{\mathbf{k}\mathbf{k}'j\lambda}$ from (2.8c). As we shall see later, when one observes the impurity-bound phonon by Raman scattering, its intensity is mostly determined by the phononlike content $|\,c_{\mathbf{k}\lambda}\,|^2$, with $\mathbf{k}$ equal to the wave-vector transfer of light. However, a small fraction $|\,d_{j\lambda}\,|^2$ follows the selection rule for the electronic excitation $0\rightarrow j$.[18]

The normalization of the eigenvector $\chi_{j\lambda}$ in (2.18) is determined by the normalization of the bound-phonon wave function (2.6): If one normalizes it so that there is one bound phonon λ in the volume V, then

$$1=(\varphi_\lambda,\varphi_\lambda)=\sum_{\mathbf{k}}|\,c_{\mathbf{k}\lambda}\,|^2+\sum_{j\,(>0)}|\,d_{j\lambda}\,|^2+\cdots\ . \tag{2.22}$$

When $\chi_{j\lambda}$ is expressed in terms of the orthonormal eigenvector $\xi_{j\lambda}$ as

$$\chi_{j\lambda}=N_\lambda\xi_{j\lambda}\quad\left[\sum_j\xi^*_{j\lambda'}\xi_{j\lambda}=\delta_{\lambda'\lambda}\right],$$

(2.22) means that the correct normalization factor N_λ is given by

$$1=|\,N_\lambda\,|^2\frac{\bar{\epsilon}V}{4\pi e^2}\left[\frac{1}{E_\lambda}+\frac{\hbar\omega_0}{2}\sum_{j\,(>0)}\frac{\xi^*_{j\lambda}\xi_{j\lambda}}{(E-\varepsilon_j)^2D_j^2}+\cdots\right], \tag{2.23}$$

where use is made of (2.20) and (2.21). As we shall see in what follows, most of the contribution to the normalization integral comes from the first term on the right-hand side of (2.22), i.e., from the one-phonon part, which is inversely proportional to the binding energy E_λ, as seen in (2.23).

In summary, we have shown that once the impurity wave functions and energies are known, we can calculate the exchange integrals (2.17), and diagonalization of this matrix gives the binding energy of the bound-phonon states. Knowledge of impurity states gives also the Raman intensity due to the bound phonon, which is essentially the square of the sum of matrix elements of $e^{i\mathbf{k}\cdot\mathbf{r}}$ between impurity ground and excited states [Eq. (2.20)].

Before proceeding, let us recapitulate in our own approach the simplest case considered by Dean, Manchon, and Hopfield.[5] First, they take the hydrogenlike impurity state $|\,nLM)$, where n is the principal quantum number, L is the angular momentum, and M is its z component. Then, evidently, the exchange integral takes a form

$$X_{n'L'M',\,nLM}=\delta_{L'L}\delta_{M'M}X^{(L)}_{n'n}\ , \tag{2.24}$$

because of the spherical symmetry. This absence of mixing of L results in the existence of bound-phonon states for each angular momentum L. Next, they consider only a single excited state for each L, and hence one needs to evaluate only diagonal exchange integrals $X^{(L)}_{nn}$. These were first calculated by Heisenberg in his famous paper[19] on the helium atom. His result for $n=2$ is

$$X_{2S,2S}=\frac{2^5}{3^6}R_0\ \text{ and }\ X_{2P,2P}=\frac{2^5\cdot7}{3^8}R_0\ ,$$

where R_0 is the Rydberg constant $R_0=me^4/(2\hbar^2)=13.6$ eV. Equation (2.16) then gives binding energies for S- and P-type bound phonons:

$$E_S=\frac{\epsilon_0}{\bar{\epsilon}}\frac{(\varepsilon_{2S}-\varepsilon_{1S})\hbar\omega_0}{(\varepsilon_{2S}-\varepsilon_{1S})^2-(\hbar\omega_0)^2}\frac{32}{729}R_0^*\ , \tag{2.25a}$$

$$E_P=\frac{\epsilon_0}{\bar{\epsilon}}\frac{(\varepsilon_{2P}-\varepsilon_{1S})\hbar\omega_0}{(\varepsilon_{2P}-\varepsilon_{1S})^2-(\hbar\omega_0)^2}\frac{224}{6561}R_0^*\ . \tag{2.25b}$$

Here, R_0 is replaced by the effective Rydberg constant $R_0^*=R_0/(\gamma_1\epsilon_0^2)$, with the inverse mass ratio $\gamma_1=m/m^*$ and the static dielectric constant ϵ_0. Equations (2.25) coincide with the result of Ref. 5.

In the hydrogen case, the one-phonon amplitude (2.20) can also be obtained analytically, but without explicit calculation we can draw some important conclusions on the interaction matrix element $(0\,|\,e^{-i\mathbf{k}\cdot\mathbf{r}}\,|\,j)$, where, in our case, $|\,0)=|\,1S)$ and $|\,j)=|\,2S)$ or $|\,2P)$. Since in Raman scattering experiments, we are interested in small $\mathbf{k}$, let us expand the exponential

$$(1S\,|\,e^{i\mathbf{k}\cdot\mathbf{r}}\,|\,j)=(1S\,|\,1-i\mathbf{k}\cdot\mathbf{r}+(1/2!)(i\mathbf{k}\cdot\mathbf{r})^2-\cdots\,|\,j)\ . \tag{2.26}$$

For $|\,j)=|\,2S)$, the first term vanishes because $(1S\,|\,2S)=0$, and the second term also vanishes by parity, and therefore the nonvanishing contribution starts from $(ka)^2$, a being the Bohr radius. For $|\,j)=|\,2P)$, the second term already gives a finite contribution and Eq. (2.26) is proportional to ka. In general, $j=L$ gives (2.26) of the order of $(ka)^L$, except for $L=0$. Thus we can tell that Raman-observable bound phonons are mainly those associated with the $S\rightarrow P$ electronic excitations.[5]

III. ACCEPTOR STATES IN THE SPHERICAL MODEL

In cubic semiconductors, when spin degeneracy is neglected, the valence band is triply degenerate at the center of the Brillouin zone, and has p-like symmetry represented by the orbital angular momentum $I=1$. The spin ($S=\frac{1}{2}$) doubles this degeneracy. In the presence of the spin-orbit interaction $\lambda\mathbf{I}\cdot\mathbf{S}$, $\mathbf{J}=\mathbf{I}+\mathbf{S}$ turns out to be a good quantum number, and the fourfold $J=\frac{3}{2}$ states are split from the $J=\frac{1}{2}$ doublet by $\frac{3}{2}\lambda$. Usually, the $J=\frac{3}{2}$ subbands are higher in energy. Because of the valence-

band degeneracy, the shallow-acceptor wave function is a mixture of several subbands,[14,20] mainly of uppermost $J=\frac{3}{2}$ states, as, usually, the spin-orbit splitting λ is much larger than the acceptor binding energy. The form of the mixing terms is determined by the symmetry of the crystal, and is characterized by a few parameters.[21] Recently, Baldereschi and Lipari[15] have rewritten Luttinger's Hamiltonian in a form composed of two terms: one, of spherical symmetry, and the other, of cubic symmetry. Baldereschi and Lipari found that the spherically symmetric term is dominant in most of cubic semiconductors, and that the cubic term can be treated as a perturbation.

The acceptor Hamiltonian in the Baldereschi-Lipari representation reads

$$H_e=\frac{\gamma_1}{2m}p^2-\frac{e^2}{\epsilon_0 r}-\frac{\gamma_1}{2m}\mu(\underline{\mathbf{P}}^{(2)}\cdot\underline{\mathbf{J}}^{(2)})+H_{\rm cub}\ . \tag{3.1}$$

The first term is the kinetic-energy term with isotropic mass m/γ_1, m being the free-electron mass, and γ_1 is Luttinger's average valence-band—curvature parameter. The second term is the Coulomb potential due to the acceptor atom screened by the host crystal with static dielectric constant ϵ_0.[22] The third term describes the mixing of the valence subbands and is proportional to a dimensionless constant μ, characterizing the difference of the light- and heavy-hole band curvatures (actually, the difference is equal to $2\gamma_1\mu$). This term has a form of the "spin-orbit" coupling, and $\underline{\mathbf{P}}^{(2)}\cdot\underline{\mathbf{J}}^{(2)}$ is a scalar product of two second-rank spherical tensors $P_q^{(2)}$ and $J_q^{(2)}$ ($q=0,\pm1,\pm2$), constructed from the momentum operator $\mathbf{p}$ and the angular momentum operator $\mathbf{J}$ ($J=\frac{3}{2}$ as described above), respectively. Finally, the last term of (3.1) has cubic symmetry and describes the warping (direction dependence of the curvature) of the valence band. Usually, in semiconductors, the contribution of $H_{\rm cub}$ is at most about 20% of the spherical term, with the exception of Si.[15] Hence, $H_{\rm cub}$ is neglected hereafter.

When the spherical "spin-orbit" constant $\mu=0$, the Hamiltonian (3.1) reduces to that of the hydrogen model and states are classified according to the angular momentum L. With nonvanishing μ, L is no longer a good quantum number, and the spin-orbit term mixes different L states having $\Delta L=0,\pm2$. In this case the "total" angular momentum

$$\mathbf{F}=\mathbf{L}+\mathbf{J} \tag{3.2}$$

is still conserved, and impurity states can be classified according to F and its z component, M. Because we consider acceptor states as being derived from the $J=\frac{3}{2}$ multiplet only, their wave function can be written in the form

$$\psi_{LJFM}=\sum_{\bar{L}}|\bar{L}JFM\rangle f_{\bar{L}JF}\ , \tag{3.3}$$

where the angular ket $|\ \rangle$ denotes an angular function, and the radial part f is a function of $r=|\mathbf{r}|$ only. The sum $\bar{L}$ is taken over those states mixed by the spherical spin-orbit interaction, and there are, at most, two terms in the sum: a main part ($\bar{L}=L$) and an admixture (either $\bar{L}=L+2$ or $\bar{L}=L-2$, but not both).

Insertion of (3.3) into $H_e\psi=\varepsilon\psi$ with (3.1) gives simultaneous radial equations for the main part f ($\equiv f_L$) and the mixing g ($\equiv f_{L\pm2}$), since the angular matrix elements can be explicitly evaluated using the reduced-matrix-element technique.[23,24] For the state $S_{3/2}$, the radial equations read

$$\begin{bmatrix} \frac{d^2}{dr^2}+\frac{2}{r}\frac{d}{dr}+\frac{2}{r}+\varepsilon & -\mu\left[\frac{d^2}{dr^2}+\frac{5}{5}\frac{d}{dr}+\frac{3}{r^2}\right] \\ -\mu\left[\frac{d^2}{dr^2}-\frac{1}{r}\frac{d}{dr}\right] & \frac{d^2}{dr^2}+\frac{2}{r}\frac{d}{dr}-\frac{6}{r^2}+\frac{2}{r}+\varepsilon \end{bmatrix}\begin{bmatrix} f(r) \\ g(r) \end{bmatrix}=\underline{0}_{2\times1}\ , \tag{3.4}$$

where we have used the effective Rydberg, as in (2.25),

$$R_0^*=e^4m/(2\hbar^2\epsilon_0^2\gamma_1)\ , \tag{3.5}$$

and the effective Bohr radius,

$$a_0^*=\hbar^2\epsilon_0\gamma_1/(e^2m)\ , \tag{3.6}$$

as units of energy and length, respectively. For the P_F states ($F=\frac{3}{2},\frac{5}{2}$), one has

$$\begin{bmatrix} a_F\left[\frac{d^2}{dr^2}+\frac{2}{r}\frac{d}{dr}-\frac{2}{r^2}\right]+\frac{2}{r}+\varepsilon & -c_F\left[\frac{d^2}{dr^2}+\frac{7}{r}\frac{d}{dr}+\frac{8}{r^2}\right] \\ -c_F\left[\frac{d^2}{dr^2}-\frac{3}{r}\frac{d}{dr}+\frac{3}{r^2}\right] & b_F\left[\frac{d^2}{dr^2}+\frac{2}{r}\frac{d}{dr}-\frac{12}{r^2}\right]+\frac{2}{r}+\varepsilon \end{bmatrix}\begin{bmatrix} f(r) \\ g(r) \end{bmatrix}=\underline{0}_{2\times1}\ , \tag{3.7}$$

where (a_F,b_F,c_F) are $(1-\frac{4}{5}\mu,\ 1+\frac{4}{5}\mu,\ \frac{3}{5}\mu)$ and $(1+\frac{1}{5}\mu,\ 1-\frac{1}{5}\mu,\ \frac{2}{5}\sqrt{6}\mu)$ for $F=\frac{3}{2}$ and $\frac{5}{2}$, respectively.[15,25] The $P_{1/2}$ states are not mixed, and their radial equation is obtained by setting $a_F=1+\mu$ and $b_F=c_F=0$ in (3.7).

Exact solutions for these equations are not known (except for $P_{1/2}$), and they are solved variationally. In Ref. 15 Baldereschi and Lipari used trial functions of the Gaussian sum with 42 parameters which are not very practical when one wants to calculate matrix elements.

TABLE I. Variationally determined acceptor energies and wave functions for the lowest levels in S and P states as functions of the spherical spin-orbit—coupling parameter μ. The energy ε is in units of the effective Rydberg R_0^*. α and β are the inverses of the spatial extension of the wave functions, and are in units of inverse effective Bohr radius $(a_0^*)^{-1}$. Finally, A and B are normalized admixture coefficients between two states having $\Delta L=2$ (A^2+B^2+1). The $2P_{1/2}$ state is not mixed ($A=1, B=0$). With the exception of this $2P_{1/2}$ state, all the wave functions become more and more localized ($\alpha,\beta\to\infty$) when μ is increased, making the binding energies increase ($|\varepsilon|\to\infty$). This is because one of the valence-band masses becomes infinite at $\mu=1$.

	$1S_{3/2}$					$2P_{1/2}$	
μ	$\lvert\varepsilon\rvert$	α	β	A	B	$\lvert\varepsilon\rvert$	α
0.00	1.000	1.000		1.000	0.000	0.250	0.500
0.05	1.002	1.003	0.944	0.999	0.032	0.238	0.476
0.10	1.009	1.011	0.947	0.998	0.065	0.227	0.455
0.15	1.021	1.026	0.959	0.995	0.098	0.217	0.435
0.20	1.037	1.047	0.975	0.991	0.131	0.208	0.417
0.25	1.060	1.075	0.995	0.987	0.164	0.200	0.400
0.30	1.089	1.112	1.021	0.980	0.197	0.192	0.385
0.35	1.125	1.158	1.056	0.973	0.231	0.185	0.370
0.40	1.170	1.216	1.100	0.964	0.264	0.179	0.357
0.45	1.227	1.290	1.152	0.954	0.299	0.172	0.345
0.50	1.298	1.384	1.221	0.943	0.334	0.167	0.333
0.55	1.387	1.502	1.305	0.929	0.369	0.161	0.323
0.60	1.501	1.657	1.415	0.914	0.405	0.156	0.313
0.65	1.651	1.859	1.559	0.898	0.441	0.152	0.303
0.70	1.854	2.141	1.759	0.879	0.477	0.147	0.294
0.75	2.141	2.543	2.041	0.858	0.514	0.143	0.286
0.80	2.573	3.152	2.469	0.835	0.550	0.139	0.278
0.85	3.295	4.185	3.193	0.811	0.585	0.135	0.270
0.90	4.723	6.215	4.618	0.786	0.619	0.132	0.263
0.95	8.842	12.120	8.757	0.759	0.651	0.128	0.256

Since we shall need only the lowest states for each L, we adopted variational functions similar to those used in their earlier work,[26] exponentials multiplied by the lowest possible polynomials, which behave correctly at the origin. For the $1S_{3/2}$ state, we take

$$f(r)=A\,2\alpha^{3/2}e^{-\alpha r}\,,$$
$$g(r)=B\,2(3)^{-1/2}\beta^{5/2}re^{-\beta r}\,. \tag{3.8}$$

These contain three independent parameters: α and β are inverse Bohr radii and A and B are normalized admixture coefficients ($A^2+B^2=1$) for the main and the mixing parts, respectively. With the trial functions (3.9), Eq. (3.5) reduces to a 2×2 eigenvalue problem:

$$\begin{bmatrix} P & R \\ R & Q \end{bmatrix}\begin{bmatrix} A \\ B \end{bmatrix}=|\varepsilon|\begin{bmatrix} A \\ B \end{bmatrix}\,, \tag{3.9}$$

with

$$P=-\alpha^2+2\alpha\,,$$
$$Q=-\tfrac{7}{3}\beta^2+\beta\,, \tag{3.10}$$
$$R^2=\mu^2\frac{2^6}{3}\alpha^5\beta^5\frac{(4\alpha+\beta)^2}{(\alpha+\beta)^8}\,.$$

The eigenvalue of (3.9),

$$|\varepsilon|=\frac{P+Q}{2}+\left[\left[\frac{P-Q}{2}\right]^2+R^2\right]^{1/2}\,, \tag{3.11}$$

is to be maximized, with respect to α and β, to yield the acceptor binding energy. The eigenvector $(A,B)^T$ gives the admixture coefficients for the corresponding states.

Similarly, for the $2P_F$ states ($F=\frac{3}{2},\frac{5}{2}$), one uses trial functions for (3.7) given by

$$f(r)=A\,2(3)^{-1/2}\alpha^{5/2}re^{-\alpha r}\,,$$
$$g(r)=B\,2^{3/2}3^{-1}5^{-1/2}\beta^{7/2}r^2e^{-\beta r}\,, \tag{3.12}$$

with which energies and admixture coefficients are obtained from (3.9) and (3.11), but this time with

$$P=-a_F\alpha^2+\alpha\,,$$
$$Q=-b_F\tfrac{27}{15}\beta^2+\tfrac{2}{3}\beta\,,$$
$$R^2=c_F^2\frac{2^{11}}{3\times5}\alpha^7\beta^7\frac{(6\alpha+\beta)^2}{(\alpha+\beta)^{12}}\,,$$

instead of (3.10).

The $P_{1/2}$ states are not mixed and can be solved exactly. Especially for $2P_{1/2}$, one has

$$|\varepsilon|=[4(1+\mu)]^{-1}$$

and the radial wave function (3.12), with

$$A=1,\quad B=0\,,\quad \alpha^{-1}=2(1+\mu)\,.$$

In Table I we summarized the result of our calculations. A remarkable fact is that, with the exception of the $2P_{1/2}$ state, when μ is increased, all the wave functions

TABLE I. (*Continued*).

		$2P_{3/2}$					$2P_{5/2}$		
$\lvert\varepsilon\rvert$	α	β	A	B	$\lvert\varepsilon\rvert$	α	β	A	B
0.250	0.500		1.000	0.000	0.250	0.500		1.000	0.000
0.261	0.521	0.486	1.000	0.026	0.248	0.497	0.469	0.999	0.045
0.273	0.546	0.504	0.999	0.050	0.248	0.497	0.471	0.996	0.091
0.287	0.574	0.523	0.997	0.072	0.249	0.501	0.475	0.990	0.138
0.302	0.607	0.547	0.996	0.093	0.251	0.509	0.480	0.983	0.186
0.320	0.644	0.574	0.994	0.112	0.256	0.522	0.490	0.972	0.234
0.341	0.687	0.606	0.992	0.130	0.262	0.539	0.504	0.960	0.282
0.365	0.737	0.643	0.989	0.147	0.270	0.563	0.522	0.944	0.329
0.394	0.796	0.688	0.987	0.162	0.281	0.594	0.546	0.926	0.376
0.428	0.867	0.741	0.984	0.178	0.295	0.634	0.576	0.906	0.422
0.468	0.952	0.805	0.981	0.192	0.312	0.685	0.615	0.884	0.467
0.518	1.055	0.885	0.979	0.205	0.335	0.751	0.665	0.861	0.509
0.580	1.185	0.984	0.976	0.218	0.366	0.837	0.730	0.835	0.550
0.660	1.352	1.113	0.973	0.231	0.406	0.951	0.817	0.810	0.587
0.767	1.576	1.284	0.970	0.243	0.460	1.108	0.937	0.783	0.622
0.917	1.889	1.525	0.967	0.254	0.538	0.329	1.105	0.757	0.653
1.141	2.359	1.887	0.964	0.265	0.656	1.663	1.360	0.732	0.681
1.514	3.142	2.491	0.961	0.276	0.854	2.220	1.787	0.709	0.706
2.258	4.701	3.694	0.958	0.286	1.248	3.326	2.638	0.686	0.727
4.465	9.258	7.216	0.955	0.296	2.400	6.539	5.117	0.666	0.746

become more and more localized ($\alpha,\beta\to\infty$), making the binding energies increase, $|\varepsilon|\to\infty$. This feature, first pointed out by Baldereschi and Lipari,[15] is due to the fact that one of the valence subbands becomes flat at $\mu=1$. The $2P_{1/2}$ state, being pure, does not contain a contribution from this subband, and its energy remains finite. We shall see in the following section that this spatial localization of acceptor wave functions also results in considerable increase in exchange integrals between acceptor states, and, consequently, in deep impurity-phonon binding.

Some comments might be necessary concerning the accuracy of our variational procedure. Our trial functions (3.8) and (3.12) reproduce, for all values of μ, the result of Ref. 15 based on 42-parameter trial functions. The error is, in the "worst" case of $1S_{3/2}$, less than 1%, even at $\mu=0.9$. Sondergeld[25] uses similar trial functions with a slightly different power: For the $2P_F$ states he takes $f\sim r$ and $g\sim r^3$ instead of our choice of $f\sim r$ and $g\sim r^2$ by arguing physically that g must behave like an F function ($L=3$). We carried out our variational procedure for these wave functions, and also for the $1S_{3/2}$ state, by taking $f\sim 1$ and $g\sim r^2$, and obtained binding energies that were always shallower than those obtained by (3.8) and (3.12). The error for $1S_{3/2}$ at $\mu=0.9$ is about 20%.

IV. EXCHANGE INTEGRAL

We have seen in Sec. II that the essential quantity which determines the impurity-phonon binding energy is the exchange integral (2.17):

$$X_{ij}=(0,i\,|\,[e^2\epsilon_0 r_{12}]\,|\,j,0)\ . \tag{4.1}$$

Here, 0 is the impurity ground state, and i and j are excited states. These are now taken to be acceptor states in the spherical model explained in the preceding section. Then the ground state is $1S_{3/2}$, while the lowest excited states are $2S_{3/2}$ or $2P_F$ ($F=\frac{1}{2},\frac{3}{2},\frac{5}{2}$). Since $S_{3/2}$ is a mixture of $L=0$ and $L=2$, and the P_F are mixtures of $L=1$ and $L=3$, an argument similar to (2.26) leads one to conclude that the matrix element $(1S_{3/2}\,|\,e^{-i\mathbf{k}\cdot\mathbf{r}}\,|\,j)$ which determines the Raman amplitude is dominant for $|j)=|2P_F)$ rather than $|j)=|2S_{3/2})$. Thus we consider hereafter only these $S\to P$ excitations. Explicitly taking the ground state $|0)=|L_0F_0M_0)$ ($L_0=0,F_0=\frac{3}{2}$) and the excited states $|i)=|LF'M')$ and $|j)=|LFM)$ ($L=1,F',F=\frac{1}{2},\frac{3}{2},\frac{5}{2}$), one has, for (4.1),

$$(F_0M_0',F'M'\,|\,[e^2/\epsilon_0 r_{12}]\,|\,FM,F_0M_0)\ . \tag{4.2}$$

The ground state has four components ($M_0,M_0'=\pm\frac{1}{2},\pm\frac{3}{2}$), while the excited states have 2, 4, and 6 components for $F=\frac{1}{2},\frac{3}{2}$, and $\frac{5}{2}$, respectively. Hence, in total, there are $4\times(2+4+6)=48$ $S\to P$ excitations, and our matrix (4.2) is a 48×48 matrix. The bound-phonon states are obtained by diagonalizing this matrix.

The 48×48 matrix can, however, be block-diagonalized by physical arguments. For this purpose, it is convenient to introduce the total angular momentum

$$\mathbf{K}=\mathbf{F}+\mathbf{F}_0\ , \tag{4.3}$$

which corresponds to the total momentum change by elec-

tronic excitation, and its z component Q. Just as in the case of exchange splitting in helium atom,[27] we pass from the (M_0,M) representation to the (K,Q) representation, and our matrix (4.1) is now expressed as

$$(F_0F'K'Q' \mid [e^2/\epsilon_0 r_{12}] \mid FF_0KQ) \ . \tag{4.4}$$

Since F_0 is fixed to be $\frac{3}{2}$, according to the addition rule for (4.3), $F=\frac{1}{2}$ gives $K=1,2$ and $F=\frac{3}{2}$ gives $K=0,1,2,3$, and, finally, $F=\frac{5}{2}$ gives $K=1,2,3,4$. Now our matrix (4.4) is diagonal in K and Q since the operator $e^2/\epsilon_0 r_{12}$ is a scalar. When rearranged according to the total momentum K, (4.4) is block diagonal and apart from the Q degeneracy, the $K=0$ part is a scalar ($F=\frac{3}{2}$ only), the $K=1$ and $K=2$ blocks are three dimensional ($F=\frac{1}{2},\frac{3}{2},\frac{5}{2}$), the $K=3$ block is two-dimensional ($F=\frac{3}{2},\frac{5}{2}$), and, finally, the $K=4$ block is again a scalar ($F=\frac{5}{2}$). Considering that each K is $(2K+1)$-fold degenerate, one can check that our matrix has a dimension of $1\times1+3\times3+5\times3+7\times2+9\times1=48$, as it should.

The evaluation of the exchange integral (4.4) is greatly simplified if one exploits the spherical symmetry of the wave functions by using the reduced-matrix-element technique.[23,24] To do so, let us first make a multipolar expansion of the Coulomb potential,

$$\frac{1}{|\mathbf{r}_1-\mathbf{r}_2|}=\sum_{l=0}^{\infty}\frac{r_<^l}{r_>^{l+1}}P_l(\cos\theta_{12}) \ , \tag{4.5}$$

where $r_>$ ($r_<$) is the larger (smaller) of r_1 and r_2, and θ_{12} is the angle between $\mathbf{r}_1$ and $\mathbf{r}_2$. Now the Legendre function in (4.5) can be expressed as a scalar product of two spherical tensors of rank l, one of argument 1 and the other of argument 2:

$$P_l(\cos\theta_{12})=\frac{4\pi}{2l+1}[\underline{Y}^{(l)}(\theta_1,\varphi_1)\cdot\underline{Y}^{(l)}(\theta_2,\varphi_2)] \ .$$

Its matrix element in the coupled scheme $\mathbf{F}+\mathbf{F}_0=\mathbf{K}$ is well known[23,24] and (4.4) becomes

$$\begin{aligned}(F_0F',K'Q' \mid [e^2/\epsilon_0 r_{12}] \mid FF_0,KQ)=\delta_{K'K}\delta_{Q'Q}(-1)^{F+F'+K}\sum_{l=0}^{\infty}\frac{4\pi}{2l+1}\begin{Bmatrix}K & F' & F_0\\ l & F & F_0\end{Bmatrix}\\ \times\sum_{\substack{\bar{L}_0',\bar{L}',\\ \bar{L}_0,\bar{L}}} I^{(l)}(\bar{L}_0'F_0,\bar{L}F;\bar{L}'F',\bar{L}_0F_0)\\ \times\langle\bar{L}_0'F_0||Y^{(l)}||\bar{L}F\rangle\langle\bar{L}'F'||Y^{(l)}||\bar{L}_0F_0\rangle \ .\end{aligned} \tag{4.6}$$

Equation (4.6) expresses the exchange integral in terms of the 6-j symbol, the radial part $I^{(l)}$, and the angular part. The sum over l comes from the multipolar expansion (4.5), while the sum over $\bar{L}$'s is due to the hybridization of L, (3.3), and hence each $\bar{L}$ sum contains, at most, two terms. The angular parts in (4.6) are two *reduced* matrix elements (or *double-bar* matrix elements) of the spherical harmonics, one corresponding to the variable 1 and the other to the variable 2. The radial integral $I^{(l)}$ is explicitly given by

$$I^{(l)}(L_0'F_0',LF;L'F',L_0F_0)=\int_0^{\infty}dr_1\,r_1^2\int_0^{\infty}dr_2\,r_2^2 f_{L_0'F_0'}(r_1)f_{LF}(r_1)\frac{r_<^l}{\epsilon_0 r_>^{l+1}}f_{L'F'}(r_2)f_{L_0F_0}(r_2) \ . \tag{4.7}$$

We note that (4.6) is, in fact, diagonal in K and Q, and that the right-hand side of it is independent of Q, as we anticipated.

Now the reduced matrix elements in (4.6) are, with respect to the coupled scheme, $\mathbf{F}=\mathbf{L}+\mathbf{J}$, and since $\underline{Y}^{(l)}$ is an operator in the configuration space L and does not operate on the "spin" space J, they can further be reduced to[23,24]

$$\langle L'JF'||Y^{(l)}||LJF\rangle=(-1)^{L'+J+F+l}[(2F'+1)(2F+1)]^{1/2}\begin{Bmatrix}L' & F' & J\\ F & L & l\end{Bmatrix}\langle L'||Y^{(l)}||L\rangle \ .$$

The right-hand side of this equation contains a 6-j symbol and the reduced matrix element of $\underline{Y}^{(l)}$, the latter being well known,[23,24] is

$$\langle L'||Y^{(l)}||L\rangle=(-1)^{L'}\left[\frac{(2L'+1)(2l+1)(2L+1)}{4\pi}\right]^{1/2}\begin{bmatrix}L' & l & L\\ 0 & 0 & 0\end{bmatrix} , \tag{4.8}$$

where the last factor is the 3-j symbol with all three magnetic quantum numbers vanishing.

This is all that we need in reducing the exchange integral (4.4). When all these results are combined, we have our final expression:

TABLE II. Exchange integral matrix elements as functions of the spherical spin-orbit coupling constant μ in units of the effective Rydberg R_0^*. This matrix is diagonal in the total momentum change K, and each block designated by K has, apart from $(2K+1)$-fold degeneracy, dimensions of 1, 3, 3, 2, and 1 for $K=0$, 1, 2, 3, and 4, respectively. These submatrices are labeled by (twice) the total angular momenta $(2F',2F)$, and their elements are even or odd with respect to the interchange of F' and F, the odd case being distinguished by an asterisk (*). Note that when the heavy-light splitting μ increases, all the matrix elements involving $F=\frac{1}{2}$ (labeled 1) become smaller, and the intensity of the exchange interaction increases while shifting towards elements involving $F=\frac{3}{2}$ and $\frac{5}{2}$ (labeled 3 and 5). This is because one of the valence subbands becomes flat at $\mu=1$, causing the $F=\frac{1}{2}$ state to spatially delocalize and the $F=\frac{3}{2}$ and $F=\frac{5}{2}$ states to concentrate about the origin.

	$K=0$				$K=1$		
μ	(3,3)	(1,1)	(1,3)*	(1,5)	(3.3)	(3,5)*	(5,5)
0.00	−0.034	0.006	0.016	0.030	−0.025	0.017	0.003
0.05	−0.041	0.005	0.016	0.026	−0.030	0.018	0.003
0.10	−0.048	0.004	0.015	0.022	−0.035	0.019	0.003
0.15	−0.057	0.003	0.014	0.019	−0.041	0.021	0.003
0.20	−0.066	0.002	0.013	0.016	−0.048	0.022	0.003
0.25	−0.078	0.001	0.012	0.014	−0.056	0.024	0.004
0.30	−0.090	0.001	0.011	0.011	−0.065	0.026	0.004
0.35	−0.105	0.001	0.009	0.009	−0.076	0.028	0.004
0.40	−0.122	0.000	0.008	0.007	−0.088	0.031	0.005
0.45	−0.142	0.000	0.006	0.006	−0.102	0.034	0.005
0.50	−0.165	0.000	0.005	0.004	−0.118	0.038	0.006
0.55	−0.193	0.000	0.003	0.002	−0.138	0.043	0.007
0.60	−0.227	0.000	0.002	0.001	−0.162	0.049	0.008
0.65	−0.269	0.000	0.001	0.000	−0.192	0.056	0.009
0.70	−0.324	0.000	−0.000	−0.001	−0.230	0.066	0.011
0.75	−0.398	0.000	−0.001	−0.001	−0.282	0.079	0.014
0.80	−0.507	0.000	−0.002	−0.001	−0.359	0.098	0.018
0.85	−0.683	0.000	−0.002	−0.001	−0.482	0.130	0.025
0.90	−1.029	0.000	−0.001	−0.001	−0.726	0.193	0.039
0.95	−2.033	0.000	−0.001	−0.000	−1.433	0.376	0.078

$$(F_0F',K'Q'\,|\,[e^2/\epsilon_0 r_{12}]\,|\,FF_0,KQ)=\delta_{K'K}\delta_{Q'Q}(-1)^{2F+F'+F_0+2J+K}[(2F_0+1)(2F'+1)(2F+1)(2F_0+1)]^{1/2}$$
$$\times\sum_l \begin{Bmatrix} K & F' & F_0 \\ l & F & F_0 \end{Bmatrix} \sum_{\bar{L}_0',\bar{L},\bar{L}',\bar{L}_0} I^{(l)}(\bar{L}_0'F_0,\bar{L}F;\bar{L}'F',\bar{L}_0F_0)$$
$$\times[(2\bar{L}_0'+1)(2\bar{L}+1)(2\bar{L}'+1)(2\bar{L}_0+1)]^{1/2}$$
$$\times \begin{Bmatrix} \bar{L}_0' & F_0 & J \\ F & \bar{L} & l \end{Bmatrix} \begin{Bmatrix} \bar{L}' & F' & J \\ F_0 & \bar{L}_0 & l \end{Bmatrix} \begin{bmatrix} \bar{L}_0' & l & \bar{L} \\ 0 & 0 & 0 \end{bmatrix} \begin{bmatrix} \bar{L}' & l & \bar{L}_0 \\ 0 & 0 & 0 \end{bmatrix}. \tag{4.9}$$

In this form, the exchange integral is fully reduced and expressed in terms of the "geometrical" factors (6-j and 3-j symbols determined uniquely by symmetry) and of the "physical" factor (the radial integral). The values of the 3-j and 6-j symbols can be found, for instance, in the book by Rotenberg *et al.*,[28] while the radial integrals can be analytically evaluated for our trial functions (3.8) and (3.12) (see Appendix). In the actual calculation, the following remarks might be useful. (i) With respect to the interchange of F' and F, (4.9) is even when $F'-F$ is even, and odd when $F'-F$ is odd. This is because the product of all the factors following the exponential of (-1) is symmetric in (F',F), as is easily checked by using the symmetry properties of the 3-j and 6-j symbols,[23,24] and therefore the effect of the interchange of F' and F in (4.9) is completely determined by the exponential factor. (ii) The sum over l runs over a few integers only. This is because of the triangular condition for the 3-j and 6-j symbols, and also because the 3-j symbol, as in (4.8), is nonvanishing only when $L'+l+L$ is even.[23,24] Actually, in our case, l is further limited to odd integers since $\bar{L}_0$, $\bar{L}_0'$ are even and $\bar{L},\bar{L}'$ are odd. In a typical case, $K=3$, the exchange matrix element for $F'=F=\frac{3}{2}$ is a sum of 18 terms: 9 terms for $l=1$ and 9 terms for $l=3$.

Before going into explicit evaluation of (4.9), let us consider the hydrogen limit $\mu\to 0$. In this case, since there is no mixing in L, the sum over $\bar{L}$'s contains only one term, $\bar{L}_0,\bar{L}_0'=0$ ($1S$ ground state) and $\bar{L},\bar{L}'=1$ ($2P$ excited state). This, in turn, limits the l sum to a single term, $l=1$. Then the only physical factor involved is the radial integral $I^{(1)}(0,1;0,1)=(2^5\cdot 7/3^7)R_0^*$. Using the table of 3-$j$ and 6-j symbols, we can determine analytically all the

TABLE II. (*Continued*).

		$K=2$				$K=3$			$K=4$
(1,1)	(1,3)*	(1,5)	(3,3)	(3,5)*	(5,5)	(3,3)	(3,5)*	(5,5)	(5,5)
0.017	0.022	0.020	−0.007	0.026	0.011	0.020	0.027	0.020	0.034
0.014	0.021	0.018	−0.008	0.027	0.010	0.024	0.029	0.020	0.033
0.011	0.020	0.015	−0.010	0.029	0.010	0.029	0.031	0.019	0.032
0.008	0.019	0.013	−0.011	0.031	0.009	0.034	0.033	0.018	0.031
0.006	0.018	0.011	−0.013	0.033	0.009	0.040	0.036	0.018	0.030
0.004	0.016	0.009	−0.016	0.036	0.010	0.046	0.039	0.018	0.030
0.003	0.015	0.008	−0.018	0.038	0.010	0.054	0.041	0.017	0.030
0.002	0.013	0.006	−0.021	0.041	0.010	0.063	0.045	0.017	0.030
0.001	0.011	0.005	−0.024	0.045	0.011	0.073	0.049	0.017	0.031
0.001	0.009	0.004	−0.028	0.049	0.012	0.084	0.054	0.017	0.032
0.000	0.007	0.003	−0.033	0.053	0.013	0.098	0.059	0.018	0.033
0.000	0.005	0.002	−0.039	0.059	0.014	0.114	0.066	0.018	0.036
0.000	0.003	0.001	−0.045	0.066	0.016	0.134	0.074	0.019	0.038
0.000	0.001	0.000	−0.054	0.075	0.018	0.159	0.084	0.020	0.042
0.000	−0.001	−0.000	−0.065	0.087	0.021	0.191	0.098	0.022	0.048
0.000	−0.002	−0.001	−0.080	0.103	0.026	0.235	0.117	0.025	0.056
0.000	−0.002	−0.001	−0.101	0.127	0.033	0.298	0.145	0.029	0.068
0.000	−0.002	−0.001	−0.137	0.166	0.044	0.402	0.190	0.036	0.087
0.000	−0.002	−0.001	−0.206	0.244	0.066	0.605	0.281	0.052	0.128
0.000	−0.001	−0.000	−0.407	0.473	0.130	1.195	0.547	0.097	0.247

exchange matrix elements (4.9).

For finite values of μ, (4.9) is to be evaluated numerically, and the result is shown in Table II. We have checked that, for small μ, the exchange matrix elements tend to the values analytically obtained. It is to be noted that as μ becomes larger, matrix elements involving $F=\frac{1}{2}$ become smaller and smaller, while those involving $F=\frac{3}{2}$ and $\frac{5}{2}$ become larger and larger. This is again a consequence of the band flattening at $\mu\rightarrow 1$ (see Sec. III), which causes spatial delocalization of the $F=\frac{1}{2}$ state at the same time as localization of the $F=\frac{3}{2}$ and $\frac{5}{2}$ states, and, hence, a decoupling between these two groups of states.

V. RESULTS AND DISCUSSION

We have calculated the acceptor states as a function of the spherical spin-orbit parameter μ, and the result is shown in Table I. We then calculated the exchange integrals (4.6) as a function of μ, and tabulated them in Table II. These two tables enable one to obtain bound-phonon energies for any cubic semiconductor: Using Table I one can calculate the resonance denominators (2.12), and combining them with the exchange matrix elements of Table II, one obtains the matrices (2.16) (at most, of three dimensions), whose eigenvalues are just the bind-

TABLE III. Physical parameters used in the present calculation. γ_1 is the average curvature of the valence bands. μ is the strength of spherical spin-orbit coupling. ϵ_0 and ϵ_∞ are static and high-frequency dielectric constants. $\hbar\omega_{\mathrm{LO}}$ is the longitudinal-optical-phonon energy at the Brillouin-zone center.

	γ_1[a,b]	μ[b]	ϵ_0[c,b]	ϵ_∞[d]	$\hbar\omega_{\mathrm{LO}}$ (meV)[d]
CdTe	5.29	0.844	9.7	7.3	21.1
ZnS	2.54	0.751	8.1	5.14	43.6
ZnSE	3.77	0.795	9.1	5.90	31.4
ZnTe	3.74	0.755	10.1	7.28	25.5

[a]Lawaetz, Ref. 29.

[b]Baldereschi and Lipari, Ref. 15.

[c]D. Berlincourt, H. Jaffe, and L. R. Shiozawa, Phys. Rev. **129**, 1009 (1963).

[d]E. Burstein, A. Pinczuk, and R. F. Wallis, in *The Physics of Semimetals and Narrow-Gap Semiconductors*, edited by D. L. Carter and R. T. Bate (Pergamon, Oxford, 1971).

TABLE IV. Theoretical (Theor.) acceptor energies and the effective Rydberg R_0^*, all in units of meV. The calculation has been done using the parameters listed in Table III. For ZnTe, experimental (Expt.) acceptor energies are also shown. The actual $2P_{5/2}$ state has two cubic-field-split components: Γ_8 (deeper) and Γ_7 (shallower).

		R_0^*	$1S_{3/2}$	$2P_{3/2}$	$2P_{5/2}$	$2P_{1/2}$
Theor.	CdTe	27.3	87.0	39.8	22.5	3.7
	ZnS	81.6	175.3	75.1	44.1	11.7
	ZnSe	43.6	110.0	48.5	28.0	6.1
	ZnTe	35.7	77.6	33.3	19.5	5.1
Expt.	ZnTe:Li[a]		58.3	20.7	13.5, 7.7	
	ZnTe:Li[b]		60.5	22.7	16.0, 10.4?	
	ZnTe:P[a]		60.2	20.6	13.7, 7.2	
	ZnTe:P[b]		63.5	23.7	17.3	7.6

[a]Nakashima *et al.*, Ref. 30.
[b]Venghaus and Dean, Ref. 8.

ing energies.

In Table III we summarize relevant physical parameters for several group-II–IV compounds. The valence-band parameters are those of Lawaetz.[29] Table IV gives calculated acceptor energies for these semiconductors. We also show in this table observed acceptor energies for ZnTe taken from Refs. 30 and 8. Experimental values by these two groups coincide well when one takes into account the difference in estimated absolute value of the $1S_{3/2}$ energy. The fact that Lawaetz's parameters give theoretical acceptor energies too deep led some authors[31,30] to readjust the band-structure parameters so that they reproduce experimental acceptor energies. We are not in a position to discuss the choice of the Luttinger parameters here,[32] and shall return to this problem concerning the acceptor–LO-phonon binding energies later. Finally, in Table V, our predictions for bound-phonon energies in ZnS, ZnSe, ZnTe, and CdTe are presented. There is no bound state for $K=0$. Bound phonons with total momentum change $K=1$ and $K=2$ have energies too small (<0.01 meV) to be observed. The $K=3$ state has two components and, as we shall see below, the deeper one is mainly associated with the $1S\rightarrow 2P_{3/2}$ excitation, the shallower one with $1S\rightarrow 2P_{5/2}$. Finally, the $K=4$ bound state has about half of the binding energy of the $K=3$ shallow state.

Regarding experiments, there seem to exist two reports so far,[33] and they are summarized in the second entry of Table V: one is by Venghaus and Dean,[8] the other by Jain *et al.*[9] The former authors find a peak between the TO and LO phonons in luminescence-excitation spectra of Li- and P-doped ZnTe. The peak at 2.6 meV below the LO phonon (called $\bar{d}$ by them) is of impurity origin, and, although they suggest the local dielectric effect (in which we are interested), they point out that in order to obtain reasonable values of theoretical binding energy one must have much stronger Fröhlich coupling than expected. Jain and co-workers[9] also observed impurity-related phonon states by Raman scattering from ZnTe:Li. They found two peaks between the LO and TO phonons, one at 2.5 meV and the other at 1.6 meV below the LO-phonon line, and infer that the deeper one is an "impurity mode" (whose nature is left unexplained) and assign the shallower one as the acceptor-bound phonon. They also calculate the impurity-phonon binding energy associated with the $1S\rightarrow 2P$ excitation in the hydrogen model [i.e., using (2.25b)] to obtain 1.0 meV and claim fair agreement with the shallow peak at 1.6 meV.

Having completed an exhaustive analysis of the acceptor-bound phonons, we are in a position to circumvent all these difficulties. We do not need to have strong electron-phonon coupling to obtain reasonable binding-energy values: In contrast to the donor-bound phonons, the non-hydrogen-like character of the acceptor states results in strong spatial localization of the wave function, an increase in exchange integrals, and, consequently, in large acceptor-phonon binding energies. The appearance of doublet structure[9] is also due to the valence-band structure effect. Thus we may conclude that the peak of Venghaus and Dean at 2.6 meV and the deeper peak of Jain *et al.* at 2.5 meV are the bound phonon with total momentum change $K=3$ mainly associated with

TABLE V. Calculated (Calc.) and experimental (Expt.) binding energies. All quantities are in units of meV. The calculation has been done using the parameters listed in Table III. Bound phonons associated with acceptor excitations $1S_{F_0}\rightarrow 2P_F$ ($F_0=\frac{3}{2}$, $F=\frac{1}{2},\frac{3}{2},\frac{5}{2}$) are classified according to the total momentum change $\mathbf{K}=\mathbf{F}+\mathbf{F}_0$ ($K=0,1,2,3,4$). There is no bound state for $K=0$. The $K=1$ and $K=2$ bound states have binding energies less than 0.01 meV in all cases and are not shown here.

		$K=3$	$K=4$
Calc.	CdTe	1.6, 0.5	0.3
	ZnS	4.4, 2.0	1.0
	ZnSe	5.4, 1.9	0.9
	ZnTe	2.2, 0.8	0.4
Expt.	ZnTe:Li,P[a]	2.6	
	ZnTe:Li[b]	2.5,1.6	

[a]Venghaus and Dean, Ref. 8.
[b]Jain *et al.*, Ref. 9.

$1S_{3/2} \rightarrow 2P_{3/2}$ (deeper one), while the second peak at 1.6 meV is that associated with $1S_{3/2} \rightarrow 2P_{5/2}$ (shallower one). As for numerical values, while calculated binding energy for the deeper state, 2.2 meV, is in reasonable agreement with experimental value of 2.6 meV,[34] the theoretical value of 0.8 meV for the shallower state agrees rather poorly with the experimental value of 1.6 meV. We shall see below that the cubic term neglected so far in the acceptor Hamiltonian (3.1) deepens this state and disagreement is removed, at least partially. A further source of discrepancy may be the choice of the valence-band parameters. We shall return to this problem at the end of this section.

It is interesting to examine in some detail the wave function for the bound phonon, (2.6). As was shown in detail in Sec. II, it can be easily calculated from the eigenvector $\chi_{i\lambda}$ in (2.18). In our case of the $K=3$ bound-phonon doublet—mixture of two electronic excitations $j=\frac{3}{2}$ $(1S \rightarrow 2P_{3/2})$ and $j=\frac{5}{2}$ $(1S \rightarrow 2P_{5/2})$—the deeper state has its electronic amplitude (2.21) given by $(d_{3/2}, d_{5/2}) \propto (0.92, -0.39)$, i.e., it is mostly $2P_{3/2}$ excitation. On the other hand, the shallower state has $(d_{3/2}, d_{5/2}) \propto (0.47, 0.88)$, and is mostly $2p_{5/2}$ excitation. The one- and two-phonon amplitudes $c_{\mathbf{k}}$ and $f_{\mathbf{k}\mathbf{k}'j}$ can also be easily calculated. Especially interesting are the phonon and electron contents in (2.22) or (2.23), and our $K=3$ deeper bound phonon can be shown to consist of 89.0% LO-phonon, 9.4% $2P_{3/2}$ electronic excitation, and 1.6% $2P_{5/2}$ electronic excitation. The contribution of the two-phonon state is negligibly small ($\sim 0.2\%$). In this way, one can draw some conclusions about the selection rules when observing the bound phonons by Raman scattering. Since they are mostly LO phonon, they follow principally the selection rules for the LO-phonon line.[18] Only in a geometry where this LO phonon is extinguished, might one find the remaining electronic part with its own selection rule.

Let us discuss some effects on impurity-bound phonons not taken into account in our theory. First, in calculating the acceptor states we have neglected the cubic term. In ZnTe, the strength of this term is approximately 20% of the spherical term.[15] The principal effect of this term[35] is the splitting of the $P_{5/2}$ states into Γ_7 and Γ_8 components. The ground state $1S_{3/2}$ and the excited states $2P_{1/2}$ and $2P_{3/2}$ are not affected to the first order, but the inclusion of higher-order coupling shifts them, particularly the $2P_{3/2}$ state because of its proximity to the $2P_{5/2}$ (Γ_8).[36] It is then to be expected that the $K=3$ bound-phonon state turns out to have three components instead of two: one is the slightly-shifted-down, deeper ($2P_{3/2}$-like) line and the other two are the shallower ($2P_{5/2}$-like) line split in two. Let us estimate this splitting. The binding energy is determined by (2.16), which is a product of the resonance denominators (2.12) and the exchange integral (2.17). The change in resonance denominator is easily obtained using the acceptor-energy values for $2P_{5/2}$ (Γ_7) and $2P_{5/2}$ (Γ_8) in Ref. 36. As for the exchange integral, we neglect nondiagonal matrix elements, which are always smaller than diagonal ones because of smaller overlap, and regard each bound-phonon state as being associated with a definite acceptor state. Then the cubic-field effect is well represented by multiplying a factor $\varepsilon(\text{cub})/\varepsilon(\text{sph})$, where $\varepsilon(\text{cub})$ and $\varepsilon(\text{sph})$ are the relevant acceptor energy with and without cubic field. In the concrete case of our Γ_8-like component of the $2P_{5/2}$-like bound phonon, the resonance denominator is 0.76, in place of the spherical value of 0.74. The exchange integral is to be multiplied by $\varepsilon_{\Gamma_8}/\varepsilon_{2P_{5/2}} = 22.3/19.5 = 1.14$. Hence, the binding energy, increased by a factor $(0.76/0.74)^2 \times 1.14$, becomes 1.0 meV. Similarly, one estimates the Γ_7-like phonon binding energy to be 0.6 meV. We believe that the $2P_{3/2}$-like line (2.2 meV) and the Γ_8-like component of the $2P_{5/2}$-like line (1.0 meV) are what is actually observed experimentally (2.5 and 1.6 meV). The Γ_7-like component (0.6 meV) may be too close to the bulk LO-phonon peak to be resolved.

The next problem is the allowance for the individual impurity species, which is experimentally known to be important in case of donor-bound phonons in GaP.[5] In p-type ZnTe, Li and P are known to be shallow acceptors, while As forms a rather deep acceptor.[30] This difference in impurity species must be reflected in the difference in acceptor-bound phonons. In fact, Venghaus and Dean have reported quite distinct impurity-related phonon states in ZnTe:As as compared to ZnTe:Li and ZnTe:P. Let us try to explain this difference. This requires, of course, to go beyond the effective-mass approximation employed in obtaining the acceptor states, and is by no means trivial. One can, however, estimate its effect in a fashion similar to the cubic-field effect by separately considering the resonance denominator (2.12) and exchange integrals (2.17). In general, the central-cell correction deepens the ground state and, hence, the resonance becomes less prominent and able to diminish (2.12), while the exchange integral is expected to increase because of the shrinkage of the wave functions. The two effects partially cancel, and the degree of this partial cancellation depends crucially on the "distance" from the resonance. In ZnTe, because of our choice of Lawaetz's parameters, the $1S \rightarrow 2P_{3/2}$ excitation has a resonance denominator of 0.93 when effective-mass energies are used, but experimental (hence central-cell-corrected) energies yield values of 1.07 and 0.80 for P and As, respectively. The change in exchange integral is accounted for by a factor $\varepsilon_{1S}^{\text{expt}}/\varepsilon_{1S}^{\text{theor}}$, with the effective-mass value $\varepsilon_{1S}^{\text{theor}} = 77.6$ meV and the experimental values $\varepsilon_{1S}^{\text{expt}} = 63.5$ and 79.0 meV for P and As, respectively. Using these values, one can identify the shift of the effective-mass bound-phonon energy (2.2 meV) to 2.4 and 1.7 meV for P- and As-bound phonons, respectively. These estimates are to be compared with the observed values, 2.6 meV in ZnTe:P (called $\bar{d}$ by Venghaus and Dean) and 0.7 meV in ZnTe:As (called d''), respectively.[37] Thus, agreement for the shallow-acceptor-bound phonon (ZnTe:P) is further improved, while one can at least account for the tendency (decrease) of the binding energy for deep-acceptor-bound phonons (ZnTe:As).

A comment may be necessary on theoretical predictions when sets of parameters other than Lawaetz's are used. With the parameters proposed by Nakashima *et al.*,[30] one obtains binding energies of 3.7 and 1.1 meV for the $K=3$ doublet. This somewhat too large binding energy is due to

the fact that their parameters give acceptor states shallower than others, and, consequently, the resonance factor may be overestimated. On the other hand, with the parameters of Venghaus *et al.*,[32] one obtains 1.8 and 1.1 meV. Their parameters seem somewhat interesting since, with them, theory gives approximately 70% of the observed binding energies for *both* deep and shallow components of the $K=3$ doublet. However, when further central-cell correction is taken into account using their parameters, binding becomes shallower (1.5 and 1.0 meV for P- and As-bound $K=3$ deeper phonons, respectively) and the discrepancy increases. We thus judged it premature to choose among alternatives a single preferable set. This is why we remained with Lawaetz's set throughout the paper and tried to force a theory without adjustment to confront the experiments. It is to compensate for this, however, that we have presented in Tables I and II all the necessary ingredients that readers themselves can use to obtain bound-phonon energies for their own parameter set without further calculation.

Finally, we wish to emphasize that our transparent formalism for impurity—LO-phonon binding is applicable not only to acceptors, but to any electronic system having several almost equal excitation energies comparable to the LO-phonon energy, including donors with valley degeneracy.

VI. SUMMARY

We have shown that when an impurity electron has several excited levels at energies comparable to the longitudinal-optical phonons, there arises a resonant coupling between the two systems, and bound states may occur. The binding energy is essentially determined by the exchange integrals among impurity electronic states. Our theory is then applied to the calculation of acceptor—LO-phonon binding energies. The valence-band degeneracy was fully taken into account using the spherical model of Baldereschi and Lipari, which then permitted us to calculate the exchange matrix elements systematically using the irreducible-tensor technique. Complications in acceptor spectra due to valence-band degeneracy is also reflected in acceptor-bound phonons, which have deeper binding energies than donor-bound phonons and fine structures classified according to the total momentum change K. We have also examined the cubic-field effect and estimated the central-cell correction. Based on our theoretical results, we have carefully analyzed experimental observations in ZnTe and established firm interpretation of impurity-related lines.

ACKNOWLEDGMENTS

We are grateful to Professor R. J. Elliott for his interest in this work. It is a pleasure to thank M. Jouanne and M. Scagliotti for discussions on their experimental results on p-type ZnTe.

APPENDIX: RADIAL INTEGRALS

The radial integral (4.7) can be analytically expressible for variational function (3.8) or (3.12), which are of the form of an exponential multiplied by a power of r. In this case we need essentially integrals of the type

$$I=\int_0^\infty dr_1 \int_0^\infty dr_2\, r_1^\lambda r_2^\mu \frac{r_<^l}{r_>^{l+1}} e^{-\alpha r_1-\beta r_2} . \tag{A1}$$

Here, as before, $f_>$ ($r_<$) is the larger (smaller) of r_1 and r_2, and hence we separate the integral into two parts, $r_1<r_2$ and $r_1>r_2$, and then use the defining integral for the incomplete Γ function,[38]

$$\int_0^x dt\, e^{-\alpha t} t^{\nu-1}=\alpha^{-\nu}\gamma(\nu,\alpha x) ,$$

to carry out the finite integrals. Then, the remaining infinite integrals are evaluated using[38]

$$\int_0^\infty dt\, e^{-\beta t} t^{\mu-1}\gamma(\nu,\alpha t) = \frac{\alpha^\nu \Gamma(\mu+\nu)}{\nu(\alpha+\beta)^{\mu+\nu}} F(1,\mu+\nu,\nu+1;\alpha/(\alpha+\beta)) ,$$

where $F(a,b,c;z)$ is the Gauss hypergeometric function.[39] The final result reads ($\kappa\equiv\lambda+\mu+1$)

$$I=\frac{\Gamma(\kappa)}{(\alpha+\beta)^\kappa}\left[\frac{1}{\lambda+l+1}F(1,\kappa,\lambda+l+2;\alpha/(\alpha+\beta)) + \frac{1}{\mu+l+1}F(1,\kappa,\mu+l+2;\beta/(\alpha+\beta))\right] . \tag{A2}$$

The first term comes from $r_1<r_2$, and the second from $r_1>r_2$. The hypergeometric functions in (A2) have arguments in (0,1) and can be most easily calculated by the series expansion.[39]

*Present address: Centre de Physique Théorique, Ecole Polytechnique, F-91128 Palaiseau, France.

†Associé au Centre National de la Recherche Scientifique.

[1] A. Mooradian and G. B. Wright, Phys. Rev. Lett. **16**, 999 (1966); A. Mooradian and A. L. McWhorter, in *Light Scattering Spectra of Solids*, edited by G. B. Wright (Springer, New York, 1969), p. 297.

[2] Y. Toyozawa and J. Hermanson, Phys. Rev. Lett. **21**, 1637 (1963).

[3] See, for a review, A. A. Maradudin, E. W. Montroll, G. H. Weiss, and I. P. Ipatova, *Theory of Lattice Dynamics in the Harmonic Approximation*, 2nd ed. (Academic, New York, 1971), Chap. 8.

[4] S. M. Kogan and R. A. Suris, Zh. Eksp. Teor. Fiz. **50**, 1279 (1966) [Sov. Phys.—JETP **23**, 850 (1966)].

[5] P. J. Dean, D. D. Manchon, Jr., and J. J. Hopfield, Phys. Rev. Lett. **25**, 1027 (1970).

[6] A. S. Barker, Jr., Phys. Rev. B **7**, 2507 (1973).

[7] D. C. Reynolds, C. W. Litton, and T. C. Collins, Phys. Rev. B **4**, 1868 (1971).

[8] H. Venghaus and P. J. Dean, Phys. Rev. B **21**, 1596 (1980).

[9] K. P. Jain, S. Nakashima, M. Jouanne, E. Amzallag, and M. Balkanski, Solid State Commun. **33**, 1079 (1980).

[10] É. I. Rashba, Pis'ma Zh. Eksp. Teor. Fiz. **15**, 577 (1972) [JETP Lett. **15**, 411 (1972)]; É. I. Rashba, Zh. Eksp. Teor. Fiz. **71**, 319 (1976) [Sov. Phys.—JETP **40**, 166 (1976)].

[11]J. Mahanty and V. V. Paranjape, Phys. Rev. B **10**, 2596 (1974).

[12]Y. B. Levinson and É. I. Rashba, Rep. Prog. Phys. **36**, 1499 (1973).

[13]M. V. Klein, in *Light Scattering in Solids,* edited by M. Cardona (Springer, Berlin, 1975), p. 147.

[14]W. Kohn, in *Solid State Physics,* edited by F. Seitz and D. Turnbull (Academic, New York, 1957), Vol. 5, p. 257.

[15]A. Baldereschi and N. O. Lipari, Phys. Rev. B **8**, 2697 (1973).

[16]M. A. Kanehisa, M. Balkanski, and R. J. Elliott, J. Phys. Soc. Jpn. Suppl. A **49**, 699 (1980).

[17]H. Fröhlich, Adv. Phys. **3**, 325 (1954).

[18]We have thus clarified the "paradox," "anomaly," and "peculiar selection rule" in Ref. 5. The authors should have introduced, in addition to $\psi_{\mathbf{k}}$ (our $c_{\mathbf{k}}$), the electronic amplitude (equivalent to our d_j), which would determine the "elementary selection rules appropriate to its symmetry (S or P)." That the "observed local mode apes the characteristic scattering behavior of LO phonon instead of having selection rules appropriate for an S or P local mode" is a straightforward consequence of the fact that the phonon amplitude $c_{\mathbf{k}}$ is dominant over the electronic amplitude d_j.

[19]W. Heisenberg, Z. Phys. **39**, 499 (1926).

[20]C. Kittel and A. H. Mitchell, Phys. Rev. **96**, 1488 (1954).

[21]J. M. Luttinger and W. Kohn, Phys. Rev. **97**, 869 (1955); G. Dresselhaus, A. F. Kip, and C. Kittel, *ibid.* **98**, 368 (1955); J. M. Luttinger, *ibid.* **102**, 1030 (1956).

[22]W. Kohn, Phys. Rev. **105**, 509 (1957); **110**, 857 (1958).

[23]A. R. Edmonds, *Angular Momentum in Quantum Mechanics,* 2nd ed. (Princeton University Press, Princeton, N. J., 1960).

[24]L. D. Landau and E. M. Lifshitz, *Quantum Mechanics,* 3rd ed. (Pergamon, Oxford, 1977), Chap. 14.

[25]M. Sondergeld, Phys. Status Solidi B **81**, 253 (1977).

[26]N. O. Lipari and A. Baldereschi, Phys. Rev. Lett. **25**, 1660 (1970).

[27]See, for instance, H. A. Bethe and E. E. Salpeter, *Quantum Mechanics of One- and Two-Electron Atoms* (Springer, Berlin, 1957).

[28]M. Rotenberg, R. Bivins, N. Metropolis, and J. K. Wooten, *The 3-j and 6-j Symbols* (Technology Press, Massachusetts Institute of Technology, Cambridge, Mass., 1959).

[29]P. Lawaetz, Phys. Rev. B **4**, 3460 (1971).

[30]S. Nakashima, T. Hattori, P. E. Simmonds, and E. Amzallag, Phys. Rev. B **19**, 3045 (1979).

[31]D. C. Herbert, P. J. Dean, H. Venghaus, and J. C. Pfister, J. Phys. C **11**, 3641 (1978).

[32]A comparative table of valence-band parameters for ZnTe is found in H. Venghaus, B. Jusserand, and G. Behnke, Solid State Commun. **33**, 371 (1980).

[33]After this work was completed, some experimental works on ZnSe:Li have come to our attention. Tews, Venghaus, and Dean [Phys. Rev. B **19**, 5178 (1979)] have observed a peak between TO and LO phonons in luminescence excitation spectra. Their suggestion of its being an impurity-bound phonon is supported by Tews, Neu, and Jiang [Phys. Rev. B **24**, 7321 (1981)], who showed the strong temperature dependence of its intensity compared to crystal phonons. The position of this line, 4.3 meV below the LO phonon, is in reasonable agreement with our theoretical prediction of 5.4 meV for $K=3$.

[34]In case of binding to hydrogenlike impurities, theory gives approximately two-thirds of the observed binding energies; see Ref. 5.

[35]See, for example, in Ref. 24, the problem in Sec. 99; we use, however, the notation of G. F. Koster, J. O. Dimmock, R. G. Wheeler, and H. Statz [*Properties of the Thirty-two Point Groups* (Massachusetts Institute of Technology, Cambridge, Mass., 1963)].

[36]A. Baldereschi and N. O. Lipari, Phys. Rev. B **9**, 1525 (1974).

[37]In As-doped ZnTe, there is another line at about 21.9 meV, called d' by Venghaus and Dean, Ref. 8, which falls below the TO phonon. Contrary to their assertion, this line is *not* the magnetic-field-dependent line at 20.1 meV observed by Scott *et al.* [Phys. Rev. B **19**, 3053 (1979)]. The suggestion by Venghaus and Dean that d' is the LO phonon very deeply bound to the As acceptor due to the fact that the $1S\rightarrow 2P_{3/2}$ excitation energy is almost equal to $2\hbar\omega_{\mathrm{LO}}$ is not very convincing, since this resonance should lead to an anomaly near $2\hbar\omega_{\mathrm{LO}}$ or in the spectral region of 52 meV. The origin of the d' line is to be found elsewhere.

[38]I. S. Gradshteyn and I. M. Ryzhik, *Table of Integrals, Series and Products* (Academic, New York, 1980).

[39]See Ref. 24, Appendix e.